# Using resource based slicing to capture the intermittency of variable renewables in energy system models

**Article** *in* Energy Strategy Reviews · December 2017

DOI: 10.1016/j.esr.2017.09.008



Mariliis Lehtveer
Linköping University

Energy Strategy Reviews 18 (2017) 73–84

Contents lists available at ScienceDirect

Energy Strategy Reviews

journal homepage: www.ees.elsevier.com/esr

# Using resource based slicing to capture the intermittency of variable renewables in energy system models

Mariliis Lehtveer*, Niclas Mattsson, Fredrik Hedenus

*Physical Resource Theory, Chalmers University of Technology, SE-412 96, Gothenburg, Sweden*

A R T I C L E I N F O

*Article history:*
Received 12 April 2017
Received in revised form
16 June 2017
Accepted 12 September 2017

*Keywords:*
Variability
Renewable energy sources
Energy system model
Time slices
Resource based slicing

A B S T R A C T

As the share of wind and solar power is expected to grow significantly in coming decades, it has become increasingly important to account for their intermittency in large-scale energy system models and global integrated assessment models that are used to explore long term developments. However, the scope of these models often prohibits the use of a high intra-annual time resolution that can adequately capture the main characteristics of variable renewables. A more efficient representation is required. In this paper we evaluate resource-based slicing, i.e. selecting time slices based on wind and solar generation rather than e.g. season and time-of-day. We show that resource slicing can capture many aspects introduced by variable renewables such as the need for flexible generation capacity, curtailment at high penetration levels and interactions with baseload and storage technologies, while using only sixteen intra-annual time slices.



## 1. Introduction

If global warming is to be kept under 2 °C with reasonable certainty, greenhouse gas (GHG) emissions must drop by roughly half by mid-century compared to current levels and continue to decline afterwards [1]. The power system is one of the main sources of emitted anthropogenic GHGs, accounting for about 30% of the total emissions [2], and therefore one of the main targets for emission reductions. Many possibilities exist for supplying energy with low lifecycle emissions such as the use of biomass, wind, solar, hydro or nuclear power. Solar and wind power have a vast physical resource potential but only supply a small share of current global energy production due to historically high costs [3]. However, recent years have seen large cost reductions for both wind and solar photovoltaic (PV) technologies, which has resulted in (and been caused by) an explosive growth of installed capacity [4]. It appears very likely that these technologies will play a major role in the future electricity system if the 2-degree target is to be met.

Yet large scale expansion of wind and solar power brings along another set of challenges. The supply from wind and solar PV technologies is variable in both short and long term and not reliably predictable. Large amounts of wind and solar power complicate systems operation by changing the residual load shape, increasing the uncertainty of supply and the need for reserve capacity. If significant amounts of intermittent capacity are installed in the system, there may be an oversupply of electricity on windy and sunny days, which is likely to result in low or even negative electricity prices. This in turn will diminish revenues for variable renewables as electricity prices tend to be low when they are able to produce electricity, and also for baseload due to decreased utilization and increased ramping. Thus solar and wind generation will have a large influence on all investment decisions and on the total cost of the system. This effect will become more acute with increasing penetration of wind and solar power.

Long-term energy models representing multiple sectors and regions are often used to investigate the questions related to long term developments such as decarbonisation of the energy system. These models typically make a cost-effective choice among large number of technologies and optimise investment decisions over many time periods and over vast geographic areas. This makes these models computationally demanding and simplifications in temporal, geographic and technological detail may be necessary to maintain reasonable running times. Typically time steps of 5–10 years are used in these models [5]. However, supply from wind and solar power varies on much shorter time scales and can be difficult to capture in large-scale models.

Traditionally, models such as POLES, IMACLIM, GET [6–8] etc. have circumvented this problem by simply limiting the amount of

* Corresponding author.
*E-mail address:* mariliis.lehtveer@chalmers.se (M. Lehtveer).

http://dx.doi.org/10.1016/j.esr.2017.09.008

variable renewables to 25–30% of electricity production; a level that is widely viewed as possible to integrate into current systems without significant additional costs. This approach limits the role that variable renewables can play in scenarios designed to investigate possible pathways to global climate mitigation, and therefore model results can be misleading. Recently different approaches have been evaluated by various modelling groups to avoid this type of artificial restriction and incorporate intermittency related effects into long-term energy models. For example, Sullivan et al. use additional constraints to capture the capacity credit provided by different penetration levels of intermittent renewables as well as technology dependent flexibility coefficients to account for the increased need for back-up capacity and flexible generation as the penetration of variable renewables increases [9]. These coefficients have been derived by using a unit commitment model with limited grid [9]. Another approach has been to interlink long-term capacity expansion models with short-term dispatch models e.g. Deane et al. [10]. However, this method requires considerable effort to set up both models and ensure the convergence of their results, as well as extensive additional computational resources.

Wind and solar power, however, are not the only sources of variability in the power system – the demand for electricity is also fluctuating over time. To describe the variability of demand in large energy system models, a time slice approach is often used. This involves implementing a coarse load duration curve for electricity demand, in which hours with similar levels of demand are grouped together (typically day/night, week-day/week-end, and seasons). Attempts have been made to extend this demand-based approach to improve the treatment of variable renewable supply. For example, Ludig et al. investigate the effect of increased time resolution of traditional demand-based slicing on capturing the variability of renewables and find that higher temporal resolution helps to capture the variability of demand and solar infeed, but does not adequately represent the variability of wind generation [11]. Nahmmacher et al. propose an approach for selecting representative days i.e. consecutive time slices that represent both varying demand levels but also variable renewable supply for long term energy system models as well as summarise other attempts in that direction [5]. They find that selecting six representative days with a temporal resolution of 3 hrs sufficiently describes the characteristic fluctuations of variable generation and demand. This results in 48 time slices per model year, which may make the approach inapplicable for very large scale energy models due to high computational requirements. Poncelet et al. explore the trade-off between techno-economic and temporal detail in models and suggest based on their results that the temporal representation should be prioritised in model development [12]. In addition, they compare time slicing to the representative days approach and find that representative days can highly improve the temporal representation of the system if chosen correctly. Ueckerdt et al. explore a method using residual load duration curves that adapt to the penetration level of variable renewables [13]. This approach captures the relationship between demand and variable infeed, but requires a more complicated set up including a more detailed electricity model to estimate the parameter values that describe how the load duration curves shift with different variable renewable shares, as well as significant amount of data for accurate approximations. Additionally, this approach leads to nonlinearities that increase the computational demands even further for models that are otherwise linear.

The aim of this paper is to demonstrate an implementation based on grouping hours by solar and wind infeed that we call resource based slicing and evaluate the number of slices needed to sufficiently well capture the variability of wind and solar generation. We show that around 16 slices can be sufficient to capture aspects of variable renewables, such as need for flexible generation capacity, curtailment at high penetration levels and interactions with baseload and storage technologies.

## 2. Method

### 2.1. The GET model

We introduce resource-based slicing into the Global Energy Transition (GET) model first developed by Azar and Lindgren [14] and further developed in Hedenus et al. and Lehtveer and Hedenus [6,8]. GET is a cost minimizing “bottom-up” systems engineering model of the global energy system set up as a linear programming problem. The model was developed to study carbon mitigation strategies with an objective of minimizing the discounted total energy system cost for the period under study (in general 2000–2100) while meeting both a specified energy demand and a carbon constraint.

The model focuses on the supply side and has five end use sectors: electricity, transport, feedstock, residential–commercial heat and industrial process heat. In each sector various technologies are available to meet the demand. Technologies are described by the energy carriers they can potentially convert, and are parameterised using e.g. investment and fuel costs, efficiencies, capacity factors and carbon emissions. Demand projections are based on the MESSAGE B2 scenarios with increasing global population, intermediate levels of economic development and a stabilisation level of 450 ppm $CO_2$ by 2100 [15]. GET has a single demand node for each region and thus the electricity grid is not explicitly modelled. Transportation demand scenarios are based on Azar et al. [14] and assume faster efficiency improvements in the transport sector than in the B2 scenario. The model has perfect foresight and thus finds the least cost solution for the entire study period with a discount rate of 5%/year. Consequently, scarce resources such as oil and biomass are allocated endogenously to the sectors in which they are used most cost-effectively. The resource base for conventional energy sources was updated for this model version based on [3] and [16].

In the model version developed in this paper, GET 9.0, the world is divided into 10 regions following IIASA region definitions (except that Eastern and Western Europe have been merged into one region): North America (NAM), Europe (EUR), Pacific OECD (PAO), centrally planned Asia (CPA), the former Soviet Union (FSU), Latin America (LAM), Africa (AFR), the Middle East (MEA), South Asia (SAS) and non-OECD Pacific Asia (PAS). The countries and territories belonging to each region are listed in Appendix B.

The current version of GET has several categories of solar and wind power: PV rooftop, PV plant A, PV plant B, concentrated solar power (CSP) with storage A, CSP with storage B, onshore wind A, onshore wind B and offshore wind. The A-versions of each technology have direct access to the electricity grid, whereas the B-versions are available at larger distances from demand and therefore require additional transmission investments; the additional cost is based on [17]. All of these eight types of solar and wind power have five resource classes each. This means that our model requires data on potentials (in GW) for each technology, region and resource class. Additionally, with the introduction of our new resource slices, the model requires data on capacity factors for each technology, region, resource class and time slice. This data is automatically provided by a new global geographical information system (GIS) framework developed for this version of the model.

### 2.2. Resource based slicing

Our proposed method involves selecting model time slices primarily based on the level of wind and solar generation instead of time-of-day and season; we call this resource-based slicing. For example, a slice called "high solar, medium wind" would aggregate together all hours that are described by this label, irrespective of when during the year they occur. The slicing is performed individually for each model region. Demand variations can in principle be combined with resource slicing by including demand as a third dimension, but in this paper we simply assume that daytime electricity demand (slices with positive solar output) is 15% higher than demand at night (zero solar output) for all regions, which is in accordance with current demand patterns in Europe [18]. In this way diurnal demand variations are captured without requiring additional slices. This simplified treatment of electricity demand lets us run the model with more solar and wind slices, which enables us to perform the convergence study described below in sections 2.3 and 3.3. Differentiating between night- and daytime demands presents an improvement over some large scale energy models that have flat demand. However, since matching electricity production and demand is a key element of energy system analysis, an improved representation based on regional demand variations is a priority for the next version of our model.

*2.2.1. GIS pre-processing and slice definitions*

To estimate the resource potential and capacity factors of wind and solar technologies, datasets of wind speeds and solar insolation for 2013–2015 were retrieved from the ECMWF ERA Interim reanalysis database. We used year 2015 as a base for our analysis and years 2013–2014 to check the robustness of the results. The ECMWF datasets were chosen because the spatial and temporal resolutions ($0.75^\circ \times 0.75^\circ$ and 3 h) were sufficient for our purposes, the wind and solar data were consistent and compatible (i.e. they referred to the same year), and because they were well documented and easy to download in bulk. Additionally, ERA Interim reanalysis data has been validated using ground measurements for multiple sites e.g. [19, 20]. The raw insolation data was converted from global horizontal irradiation to global tilted irradiation for solar PV and to direct normal irradiation for solar CSP, and further converted to a time series of capacity factors by simulating the impact of thermal storage for CSP over the year. Capacity factors were produced from the wind data by combining raw wind speeds with a power curve from a typical wind turbine (Vestas 112, 3.075 MW).

Several auxiliary datasets were used to exclude areas where solar and wind power cannot be placed, and to estimate potentials for each technology, model region and resource class. The datasets include population (GPWv4, [21]), land cover (MODIS, [22]), protected areas (WDPA, [23]), and topography and bathymetry (ETOPO1, [24]). Additionally, a dataset of gridded per-capita income [25] was used as a proxy for access to electricity. After masking out unsuitable locations, a certain fraction of the remaining area is considered available for solar and wind farms. The key parameters used for this GIS analysis are listed in Appendix A. Many of these assumptions are by nature extremely uncertain, but since quantitative results are not a focus of this paper no sensitivity analysis was performed on these assumptions.

Next we allocate each 3-h time step in each model region to one of our slices. The allocation is based on the output of "representative time series" for solar PV and wind power, which are calculated by assuming that PV panels and turbines are distributed evenly throughout each region in all grid cells with above average solar or wind resources.

We test two different methods of defining slices in this paper. When we use "manual slicing", we sort the hourly output of the representative time series and divide them into a number of percentiles, depending on the number of slices. For wind power, the percentiles are distributed evenly. For solar PV, the first slice represents night-time conditions and contains the lower 50 percentiles of output. The upper 50 percentiles of output are distributed evenly among the remaining slices. The notation SxW is used to indicate the number of solar and wind slices. See Fig. 3 for sample results using $3 \times 3$ manual slicing.

Alternatively, we determine slices automatically based on k-means clustering of the two-dimensional distribution of solar and wind output of the representative time series. This selects optimal values of solar and wind output for each slice by minimizing squared Euclidean distances to the center points for each observation of three-hourly output, see Fig. A3. In other models which have time series for electricity demand or other important variables to slice on, the clustering can easily be extended to multiple dimensions. Clusters are selected using the k-means++ algorithm [26] which uses a heuristic to determine initial centroid locations. There is some randomness in the heuristic, so the algorithm is repeated 200 times for each region to find stable cluster configurations [27].

When every 3-h time period has been allocated a time slice, we calculate the average capacity factor for every combination of technology, model region, resource class and time slice. The output from this step provides the main input for the GET model. The GIS preprocessing step and slicing methods are described in greater detail in Appendix A.

*2.2.2. Implementation of slices in GET*

Adding slices to a linear programming model like GET that previously lacked intra-annual time periods involves introducing an extra set (or dimension) that all variables are indexed over. This increases the size of the model by an order of magnitude. Although electricity demand is not currently used as an input for slicing, daytime demand (i.e. slices with medium and high solar) is assumed to be 15% higher than night-time demand based on ENTSO-E 2014 data for Europe [18]. This difference is assumed to be the same for all regions.

To avoid making the model unnecessarily large, we have currently restricted the use of slices to the electricity generating sector. When other sectors interact with electricity generation, e.g. by using electricity or providing fuel for electricity generation, they do so on an annual basis only. For example, if electricity is generated from hydrogen in a particular slice, the same amount of hydrogen must be produced elsewhere, say by gasification of biomass. However, model variables representing hydrogen production from biomass are annual variables and are not disaggregated into slices. This can also be viewed as if there existed a free and 100% efficient technology for intra-annual hydrogen storage. The situation outside the electricity sector is no different from a model that lacks time slices, which some large integrated assessment models do. The standard approach in these models and in GET 9.0 is to include implied costs (for e.g. hydrogen storage) in other cost parameters of the model, and to specify exogenous capacity factors that describe average annual utilization of installed capacity when there is insufficient time resolution to treat utilization endogenously.

An additional constraint representing "aggregate part-load" is introduced to take into account start-up and ramping limitations of dispatchable technologies and restrictions on the use of hydro reservoirs. To prevent these technologies from suddenly ramping down to zero in a slice, they must always run at a minimum share of their actual output in any other time slice. These shares are displayed in Table 2. For example, if in a certain region the maximum production of coal electricity is 100 GW over all slices, then at least 50 GW of coal power must be produced in all other slices.

One limitation of using slices is that treatment of electricity storage becomes difficult when there is no chronology of intra-annual time periods. As a workaround, we retain some of this information by calculating a “slice transfer matrix” based on the time series of slice allocations. To illustrate the concept: suppose we have a 12-h storage technology and are interested in how slice X can interact with other slices. We iterate over all time periods in a year and count which other slices appear within 12 h after every occurrence of slice X. This gives an upper bound for the number of hours the storage technology can be used to transfer energy from slice X to any other slice. A similar approach has been previously explored by Wogrin et al. [28].

### 2.3. Main scenario

In this section we briefly describe the main scenario used to evaluate how well resource-based slicing captures the main characteristics of variable renewables. We selected a scenario with relatively ambitious reductions of $CO_2$ emissions and significant technological development to encourage the large-scale use of solar and wind power. In the next section, we examine aggregated global model results for this scenario and intra-annual results for individual regions and years. Additionally, to explore how many slices are required for the results to converge to a stable solution, we ran the model with 1, 2, 4, 9, 16, 25, 36, 49 and 64 slices, using both manual slicing and k-means clustering. Model runs with more than 64 slices failed due to insufficient RAM memory.

We construct mitigation pathways for all regions that meet the 450 ppm $CO_2$ target globally based on the idea of contraction and convergence [29] and with climate sensitivity of 3 °C per doubling of $CO_2$. The developed regions and emerging economies roughly halve their emissions compared to the baseline by 2050, whereas developing regions (AFR, MEA, SAS, PAS) reduce emissions by 35% compared to the baseline. From 2060 we assume a global cap, and emissions are allocated among regions in the most cost-effective way. For developing technologies, investment costs decline linearly over the 2010–2050 period and reach mature levels as indicated in Table 1.

For developing technologies, investment costs decline linearly over the 2010–2050 period and reach mature levels as indicated in Table 1. The growth of technologies is limited to a ten percent increase in installed capacity per year.

## 3. Results

### 3.1. Global and regional electricity mix

Fig. 1 displays global electricity production over the 21st century from a model run using 16 slices. By the end of the century wind and solar PV make up 42% of electricity supply. Another 20% is provided by concentrated solar power with thermal storage. Carbon Capture and Storage (CCS) technologies are not entirely carbon free in our model since only 95% of $CO_2$ emissions are captured. This explains the declining share of CCS during the last decades of the century in which the carbon budget becomes more stringent. The main competition will therefore be between nuclear, wind and solar technologies.

The energy mix varies significantly across model regions as depicted in Fig. 2. This illustrates the different resource endowments in different regions as costs in our model are uniform. In regions with good wind and solar resources such as LAM and NAM, renewables dominate. In regions with more limited resources such as SAS and PAS, nuclear power is the main technology for providing

**Table 2**
“Aggregate part-load” constraint: minimum share of maximum output in other slices.

| | Aggregate part-load |
|---|---|
| Biomass power plant | 0.5 |
| Oil power plant | 0.2 |
| Gas power plant | 0.2 |
| Coal power plant | 0.5 |
| Light water reactor | 0.7 |
| Fast breeder reactor | 0.7 |
| Hydro power plant | 0.2 |

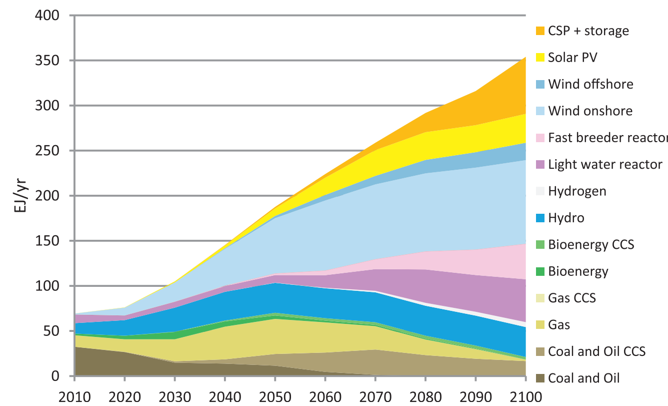


**Fig. 1.** Global electricity production mix with the 450 ppm $CO_2$ scenario and clustering with 16 slices.

**Table 1**
Investment costs of technologies in the GET model.

| Technology | Starting cost per kW ($ 2010) | Mature cost per kW ($ 2010) | Efficiency |
|---|---|---|---|
| Coal power plant | 1800 | 1800 | 45% |
| Coal power plant with CCS | 3000 | 2500 | 35% |
| Gas turbine | 800 | 800 | 55% |
| Gas turbine with CCS | 2000 | 1500 | 45% |
| Concentrated solar power (CSP) + storage A | 7000 | 4500 | N/A |
| Light water reactor | 7000 | 5000 | 33% |
| Fast breeder reactor | 8500 | 6000 | 41% |
| Wind onshore A | 2000 | 1500 | N/A |
| Wind offshore | 5000 | 3000 | N/A |
| Solar PV rooftop | 4000 | 1600 | N/A |
| Solar PV plant A | 3700 | 1250 | N/A |
| Storage 12 h | 1800 | 1800 | 80% |
| Storage 24 h | 2900 | 2900 | 80% |
| Storage 48 h | 5100 | 5100 | 80% |
| Storage 96 h | 9500 | 9500 | 80% |

Sources: [8,30,31].

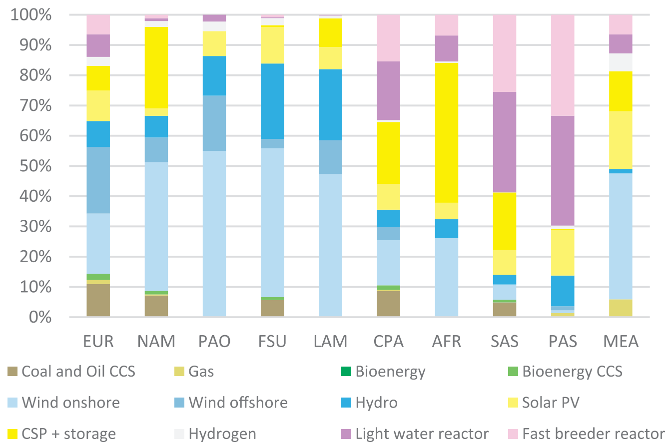


**Fig. 2.** Regional electricity production mix in year 2100 with the 450 ppm $CO_2$ scenario and 16 clusters.

electricity. Wind also tends to contribute to the electricity production to a larger extent than solar PV, with the exceptions of SAS and PAS.

### 3.2. Sliced electricity generation

Results from the GET model using 3 × 3 manual slicing are shown in Fig. 3, which depicts electricity output in Europe in 2050 in the 450 ppm scenario. The x-axis represents a full year and the width of each bar the share of hours that falls into a given slice. The unit of the y-axis is capacity (in GW), and therefore the area of each bar is the total electrical energy generated in that slice. The first three slices (s11, s12, s13) represent the lower 50 percentiles of the representative time series of solar PV generation, which will generally occur during night time. The upper 50 percentiles are equally distributed between medium solar PV output (s21, s22, s23) and high solar PV output (s31, s32, s33). The representative time series of wind power is equally distributed in thirds between low wind output (s11, s21, s31), medium wind output (s12, s22, s32) and high wind output (s13, s23, s33).

A significant amount of electricity (39%) comes from wind and solar PV in 2050 in this scenario. Onshore and offshore wind power provide roughly half of all electricity during windy conditions whereas solar PV covers most of the demand during daytime peak hours. Nuclear power, coal CCS and biomass CCS plants are run as constant baseload, providing roughly 30% of annual electricity. Gas and hydro power plants are used to compensate for the variability of wind and solar production. No significant curtailment or electricity storage is required in this case.

The combined share of variable solar and wind energy increases to 53% in 2100 with CSP additionally providing 8% of electricity. As the amount of allowed emissions becomes smaller, gas power plants can no longer be used to compensate for the variability of wind. Several other technologies contribute to manage the variations. Hydropower is ramped more aggressively than in the 2050 results, and baseload generation of coal and nuclear power is reduced when solar and wind output is high. The model "over-invests" in intermittent power to some extent, leading to significant curtailment in slice s33. Hydrogen is used to generate electricity during less windy periods in slices s11 and s21. Investments in CSP with 12 h thermal storage also take place due to the ability to provide electricity during the night. No dedicated electricity storage is used in Europe. However, electricity storage makes significant contributions in some other regions.

One important characteristic of variable production is so-called "profile costs", which depend on the temporal matching of variable renewable supply profiles with power demand. Profile costs are claimed to be the main cost impact of variable renewables above 15% penetration level [32,33] compared to e.g. grid and cycling costs. The results above demonstrate that our modelling approach using resource-based slicing captures the three main drivers of profile costs: a low capacity credit for variable renewables and resulting requirements for firm capacity, as demonstrated by low wind and solar slices where other technologies that variable renewables need to be invested in; reduced utilization of dispatchable plants as demonstrated by high wind and solar slices where dispatchable capacity is down regulated; and occasional overproduction of variable generation resulting in curtailment.

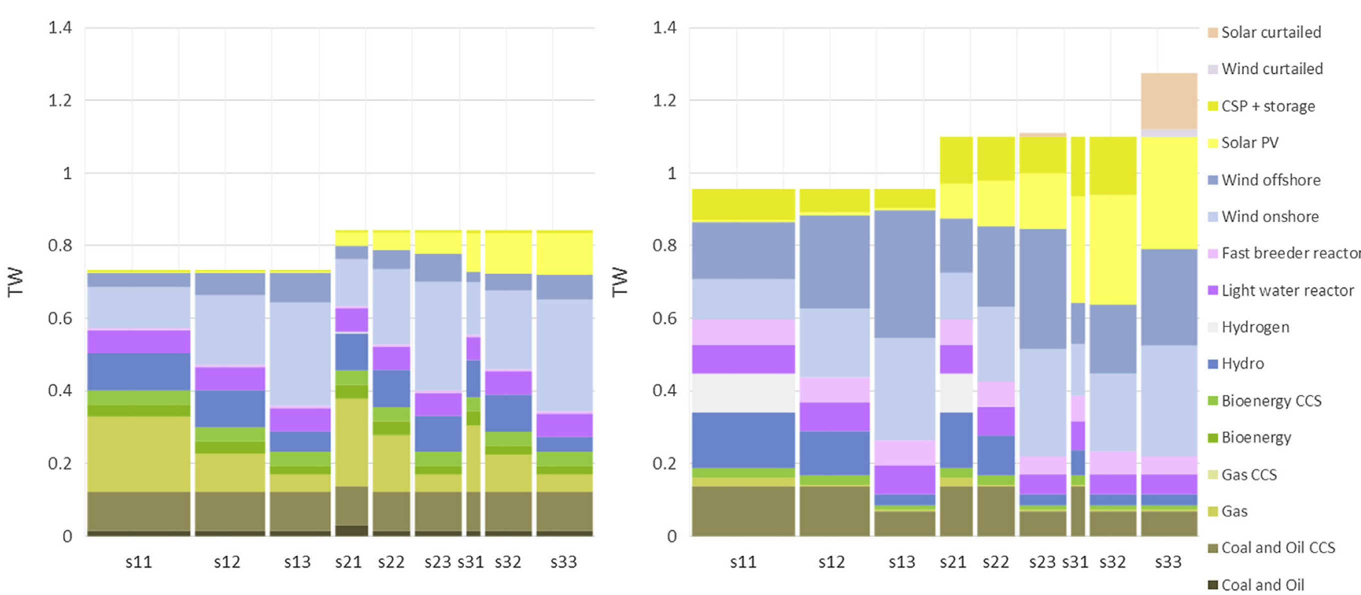


**Fig. 3.** Electricity production mix in different slices for Europe in 2050 (left) and 2100 (right) with the 450 ppm $CO_2$ scenario and 3 × 3 manual slicing. The width of each slice represents the share of hours that fall into that category.

### 3.3. Convergence and number of slices

When the model is run with only a single slice, it is equivalent to a model with no intra-annual time periods or slices without any extra constraints on allowed penetration of wind and solar power. Capacity factors for variable renewables are averaged over the year and thus all information about variability is lost. Adding a second slice introduces the day/night division and higher daytime demand. These are the main aspects of variability captured by models with traditional demand-based time slices. We therefore regard our two-slice runs as indicative of results using models with demand slicing.

The resulting global electricity mix in 2100 is shown in Fig. 4. We note that both manual slicing and clustering approaches converge quickly to solutions close to the 64-slice optimum. Clustering generally converges faster than manual slicing, but the difference is small. Single slice runs vastly overestimate optimal levels of Solar PV due to its averaged output that is treated as dispatchable in one slice model. This tendency is still present for 2 × 1 manual slicing, although wind power generation is approximately correct when two slices are employed. However, we also observe that the solution has not entirely converged even when using 49 slices, especially for manual slicing. We conclude that although 9–16 slices may provide acceptable solutions for large integrated assessment-type models, models with higher intra-annual time resolution are required to study the contribution of variable renewables in detail.

On a regional level results are as expected somewhat noisier, but generally our observation that 9–16 slices are sufficient to produce acceptable solutions remains valid (Fig. 5).

To assess the stability of our results at the regional level we looked at results from runs with 9–64 slices where global results have become rather stable. We calculated the standard deviation for each technology in this range and related these results to average demand. The outcomes are shown on Figs. 6 and 7. The standard deviation is less than 4.5% of demand in all cases, with some regions more stable than others. It is also interesting to note that stability of results in different regions depends on the method of slicing. For example, AFR has the highest variance in clustering results although it is one of the most stable regions with manual slicing. Often there is a co-variance between solar PV and CSP technologies. This may be explained by our model setup where we model CSP with 12 h thermal storage and also have a 12 h general storage technology available that is a good match for the rather regular and predictable production pattern of solar PV. Therefore small changes in input data can make the model choose one or the other. Further sensitivity analysis is needed for interpretation of quantitative results. Neither of the two methods is obviously superior based on stability of regional results, although our global results indicate that clustering converges slightly faster than manual slicing as the number of slices increases. We hypothesise that this is due to an improved approximation of the duration curve of wind and solar output in the clustering case (see Appendix A Figs. A1 and A2). On the other hand, manual slicing results are easier to interpret graphically.

## 4. Discussion

Our results show that resource-based slicing can capture characteristic aspects of variability. Although our approach is simple and uses relatively few time slices, we observe curtailment of variable renewables during high availability, the interplay of flexible and inflexible dispatchable power plants in meeting demand during low availability, and the potential benefits of storage. These essential characteristics do not emerge in models with only one time slice (e.g. previous versions of the GET model [8]) and are captured only for solar energy with demand-based slicing [11]. Thus, resource-based slicing can capture important features of a system with high penetration of variable renewables in a rather simple manner. There are, however, limitations to our method, especially when applied to models with different geographical scope.

First, trade of electricity and heat between model regions is not straightforward with resource-based slicing since slices in different regions do not generally refer to the same time periods. This is not a significant limitation for a global model with continent-sized regions, but it may be a concern for a more detailed model of e.g. Europe or the USA, with sub-regions representing individual states or relatively small countries. However, it may be possible to apply resource-based slicing to more detailed models in which interregional electricity trade plays a role, using various workarounds. One option is to slice the entire modelled area at the same time. Due to regional differences in wind and solar production at any given time this approach would result in greater averaging of wind and solar capacity factors, but it may be feasible even for a region as large as e.g. Europe. Another possible approach may be to use transition matrices to account for electricity trade similar to the ones used here to model storage. Trade of other energy carriers such as liquid fuels is not significantly affected by this restriction since it can be

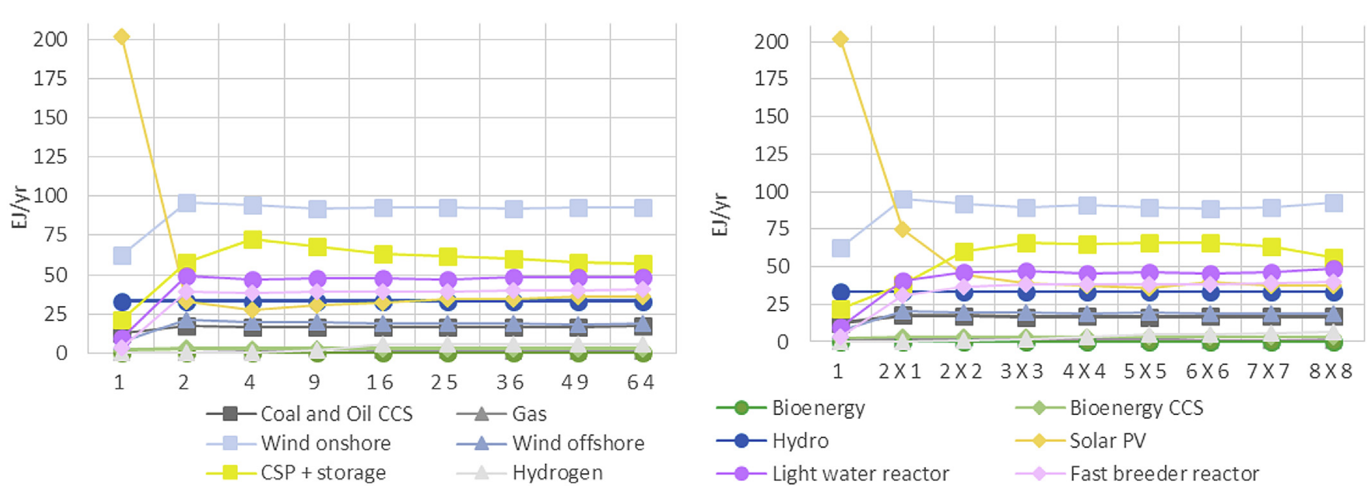


**Fig. 4.** Global electricity mix at year 2100 for different number of slices with clustering (left) and manual slicing (right).

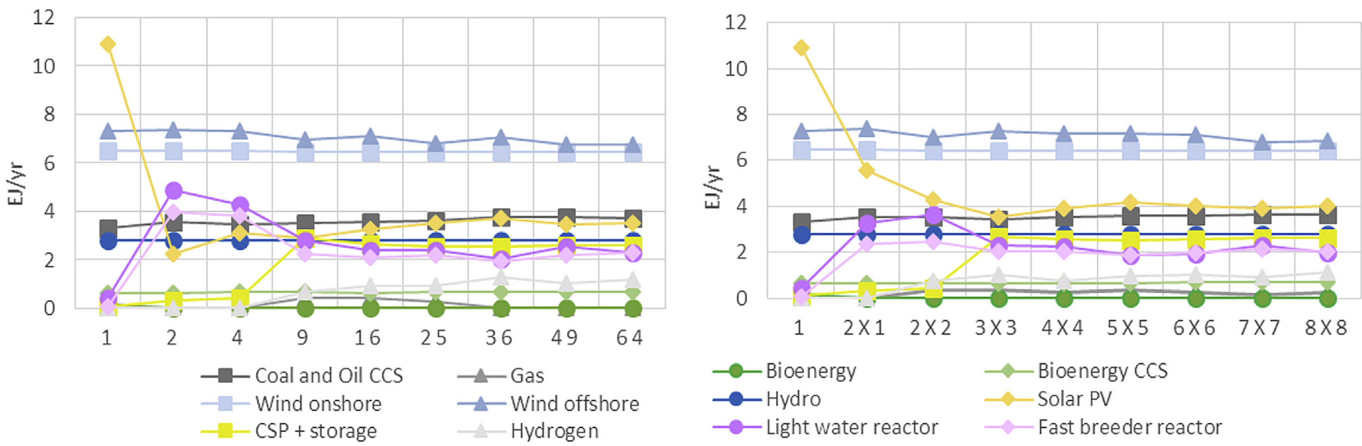


**Fig. 5.** Electricity mix at year 2100 for Europe for different number of slices with clustering (left) and manual slicing (right).

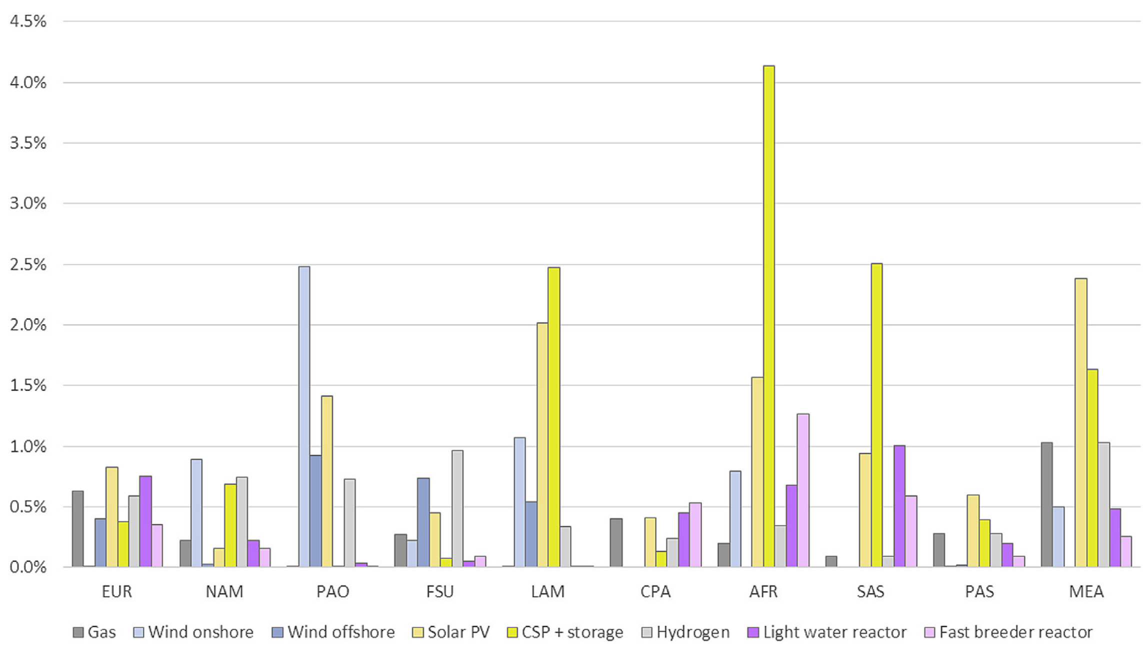


**Fig. 6.** Standard deviation of electricity generation of main technologies relative to regional demand in clustering results with 9–64 slices.

described using annual trade flows.

The second limitation is that temporal sequencing of wind and solar variability is lost when hourly output is aggregated into slices. The main effect is that it becomes more difficult to include short-term responses to renewable intermittency into the model, such as electricity storage or cycling of thermal baseload generation. We propose simple workarounds with our "slice transfer matrix" for electricity storage and "aggregate part-load" constraint (see section 2.2.2). Thermal cycling is typically not at all addressed in global models with a few recent exceptions [e.g. 9]. Our approach is a contribution in that respect. Still, to perform analysis of the electricity system at short timescales, more detailed dispatch models are likely required.

A related issue is the loss of explicit seasonal slices, which may be useful for describing e.g. hydropower availability and potential long-term storage or seasonal demand variations. Although we did not consider these effects of sufficient importance to include in our model, seasonal slices could easily be combined with resource-based slices, at the cost of a larger number of slices in the model.

Our "slice transfer matrix" is less accurate in modelling short term storage compared to the representative days approach proposed by e.g. Nahmmacher et al. [5], but may be more accurate for long-term storage. Modelling representative days or weeks can result in a very large number of time slices and thus become computationally too demanding to use in large models. However, recent studies indicate that storage may not be very important even in scenarios with high penetration of variable renewables [34,35], although this conclusion may not hold at extremely high penetration levels (90% or more).

Thirdly, demand fluctuations are not accounted for in our analysis. Ueckerdt et al. show that current demand profiles vary across world regions and are also to different degree correlated with wind and solar patterns [36]. However, if data is available, demand could be included in slice creation as another dimension (see e.g. Wogrin et al. [28]). Although this would increase computational requirements, the clustering approach could be used to

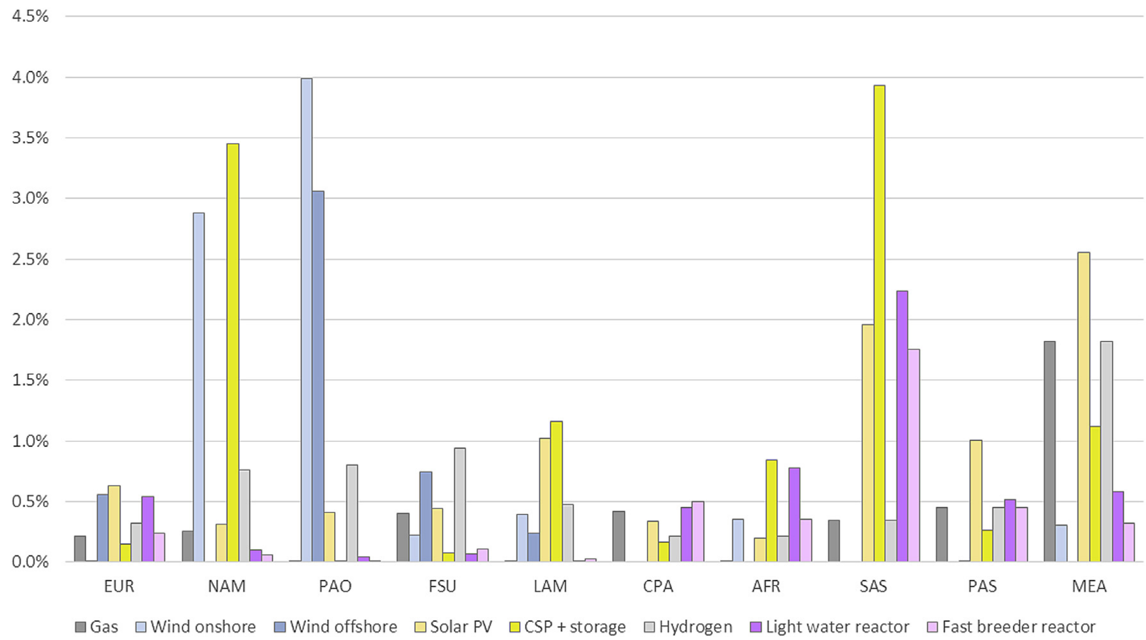


**Fig. 7.** Standard deviation of electricity generation of main technologies relative to regional demand in manual slicing results with 9–64 slices.

select slices efficiently and reduce the size of the model.

Finally, we do not explicitly model grid extensions needed for large-scale renewable penetration. Instead we assume that significant amounts of new transmission capacity are required at a uniform cost per kW in all regions. In reality this cost is likely to vary depending on the penetration of variable renewables, pre-existing infrastructure and grid design. Again, most existing global energy systems models are subject to this limitation.

## 5. Conclusions

As the share of variable renewables – wind and solar PV – is expected to grow significantly in coming decades, it has become increasingly important to account for their intermittency in large scale energy models that are used to explore long term energy futures. In this paper we propose and evaluate a method for doing so, namely, resource based slicing. By analysing global wind speed and solar insolation data we derive resource potentials for wind and solar as well as capacity factors for different availability situations in 10 world regions, and use this data as input to the Global Energy Transition (GET) model. Since even a relatively small number of resource-based slices can capture significant part of the variability of solar and wind power, this enables us to remove traditional constraints on intermittent electricity generation from the model.

Our results show that this approach can capture many aspects introduced by variable renewables such as the need for flexible generation capacity, low capacity credit for variable renewables and curtailment at high penetration levels. We note that using a simple day/night split as is common in models with traditional time slices may significantly overestimate optimum levels of solar PV. We also find optimal electricity production mixes to vary significantly between regions due to different endowments of solar and wind resources. Additionally, we compare two methods of choosing slices – manual slicing and clustering – and find that although both of them perform well, clustering converges slightly faster. We believe that clustering could outperform manual slicing to a larger extent in the three-dimensional case where slices are not only based on solar and wind resources but also on electricity demand.

Our approach is aimed at large integrated-assessment type models in which the use of a high temporal resolution to analyse variable renewables may be computationally infeasible. Resource-based slicing provides a simple way of representing important aspects of variable renewable electricity production in these models, which has previously been partly or completely lacking.

## Author contributions

FH and NM conceived the study. NM implemented resource-based slicing in the GET model and developed the GIS pre-processing framework with contributions from FH and ML. ML performed the model runs and analysed the results with contributions from FH and NM. ML and NM wrote the paper with contributions from FH. ML and NM made equal contributions overall and are listed in alphabetical order.

## Acknowledgements

We would like to thank ÅF and Chalmers University of Technology's Area of Advance Energy for funding this research project and Lina Reichenberg for her insightful comments on this work.

## Appendix A. GIS datasets and analysis

### *Solar and wind datasets*

Datasets of solar insolation and wind speeds were obtained from the ECMWF ERA Interim reanalysis [20]. Both datasets have a spatial resolution of approximately 0.7° × 0.7° at the equator and a time resolution of 3 h. Our model has been tested using datasets for

2013, 2014 and 2015, although the GIS preprocessing step and the main GET model only use one year of data at a time. The results were found to be robust for tested years.

For solar PV and concentrated solar power (CSP), we downloaded datasets for global horizontal irradiation at surface level and top-of-atmosphere from the ERA Interim database. The BRL model [37] is used to estimate the diffuse fraction using the clearness index and other variables derived from the two solar datasets, and to calculate the direct normal irradiation. This forms our main input data for CSP and the beam component of the total insolation for solar PV. CSP in the GET model is assumed to be of solar tower type, which uses two-axis tracking to follow the sun across the sky.

To estimate diffuse sky radiation for solar PV, we use the Hay-Davies model as it appears in Loutzenhiser et al. [38]. Solar PV panels are assumed to be latitude-tilted and equator-facing, and ground albedo is uniformly assumed to be 0.2. The global tilted irradiation on the PV panel is then the sum of direct normal irradiation projected onto the panel surface, the diffuse sky radiation and diffuse radiation reflected off the ground.

For wind power, we download U and V components of wind speeds at a height of 10 m from the ERA Interim database. The wind time series is then rescaled so that annual average wind speeds for every grid cell matches average wind speeds from the Global Wind Atlas [39] at 100 m height. This results in a global gridded time series that considers local topography and surface roughness.

Wind speeds are translated to instantaneous capacity factors using a power curve based on the Vestas V112 3.075 MW wind turbine. Regional wind speed variations within a grid cell are considered by smoothing the power curve by applying a convolution with a Gaussian probability density function with a standard deviation of 1 m/s [40]. Availability and electrical losses are assumed to be 6% and average wind farm wake losses at 11.5% [41].

*GIS analysis*

We used several auxiliary datasets to estimate potentials for solar and wind power, disaggregated by model region, technology type and resource class. The datasets include population (GPWv4, [21]), land cover (MODIS, [22]), protected areas (WDPA, [23]), and topography and bathymetry (ETOPO1, [24]). Additionally, a dataset of gridded per-capita income [25] was adapted to roughly approximate access to electricity by applying a lower threshold value to a spatial filter of logarithm of income. All datasets were resized to a spatial working resolution of $5 \times 5$ arcminutes for the purpose of estimating technology potentials.

The main parameter assumptions used in the GIS analysis are shown in Tables A1 and A2. The conditions concerning population density, grid access, land cover and protected areas were used as a mask to exclude entire $5 \times 5$ arcminute grid cells from the area available for solar and wind power. A small fraction of the area of the remaining grid cells in each region (listed in the "Area available" column) was considered available for solar and wind farms, and the capacity density was used to convert this area to potentials measured in GW. The distances 9 and 149 km appear as a result of our working resolution: one grid cell is roughly 9 km wide at the equator, and 16 cells are 149 km wide at the equator.

Note that capacity factors for CSP in Table A2 are considerably higher than those for solar PV. This is because CSP is assumed to include 12 h of thermal storage and a solar multiple of 2.5 (i.e. power of the solar collector field relative to the generator). A simple simulation of CSP with storage is performed for each grid cell, assuming that CSP uses its storage to run at rated capacity for as long as possible every day. This produces a time series of output from CSP and storage for every grid cell that is required in a later step of the GIS analysis.

**Table A1**
Main GIS assumptions for solar and wind potentials.

| | Capacity density *[W/m²]* | Area available after masks *[percent]* | Population Density (PD) *[persons/km²]* | Grid access (GA) *[km]* | Excluded land cover types and offshore areas | Excluded protected areas *[IUCN codes]* |
|---|---|---|---|---|---|---|
| PV rooftop class 1-5 | 45 | 4 | PD > 100 | GA < 9 | cropland | not reported, I - IV |
| PV plant class A1-A5 | 45 | 2 | PD < 75 | GA < 9 | cropland | not reported, I - IV |
| PV plant class B1-B5 | 45 | 2 | PD < 75 | 9 < GA < 149 | cropland | not reported, I - IV |
| CSP plant class A1-A5 | 35 | 2 | PD < 75 | GA < 9 | cropland | not reported, I - IV |
| CSP plant class B1-B5 | 35 | 2 | PD < 75 | 9 < GA < 149 | cropland | not reported, I - IV |
| onshore wind class A1-A5 | 5 | 5 | PD < 75 | GA < 9 | urban, wetlands | not reported, I - IV |
| onshore wind class B1-B5 | 5 | 5 | PD < 75 | 9 < GA < 149 | urban, wetlands | not reported, I - IV |
| offshore wind class 1-5 | 8 | 33 | – | GA < 149 | areas within 9 km of shore or with depth > 40 m | not reported, I - IV |

**Table A2**
Resource class definitions for solar PV and CSP in terms of annual average capacity factor (CF), and resource classes for onshore and offshore wind power in terms of annual average wind speed (AWS, m/s).

| | class 1 | class 2 | class 3 | class 4 | class 5 |
|---|---|---|---|---|---|
| solar PV | 0.10 < CF < 0.15 | 0.15 < CF < 0.20 | 0.20 < CF < 0.24 | 0.24 < CF < 0.28 | CF > 0.28 |
| CSP + storage | 0.32 < CF < 0.40 | 0.40 < CF < 0.48 | 0.48 < CF < 0.56 | 0.56 < CF < 0.64 | CF > 0.64 |
| onshore wind | 4 < AWS <5 | 5 < AWS <6 | 6 < AWS <7 | 7 < AWS <8 | AWS >8 |
| offshore wind | 5 < AWS <6 | 6 < AWS <7 | 7 < AWS <8 | 8 < AWS <9 | AWS >9 |

*Slice definitions and evaluation*

An important stage of the GIS analysis for our model is to allocate each 3-h time step in each region to one of our time slices. In order to do this, we calculate a “representative time series” for solar PV and wind power (individually) in each region. Although we do not know at the preprocessing stage which of the resource classes will be economically viable during the later linear programming stage, we assume that solar and wind power will be distributed evenly throughout all grid cells of each model region in the upper resource classes as follows. The representative time series for solar PV includes all grid cells that have PV rooftop class 3–5, PV plant class A3-A5, or PV plant class B5. The representative time series for wind power includes all grid cells that have onshore wind class A3-A5, onshore wind class B5, or offshore wind class 5. The implicit assumption is that both wind and solar energy will be installed wherever they are economically viable, instead of being concentrated in the very best locations. This assumption appears to hold for facilities that exist today. Note that slice definitions are based on entirely on solar PV or wind output, and that CSP output is not used for allocating slices.

Resource slices are calculated based on the combined output of the representative time series for solar PV and wind power using either “manual slicing” or k-means clustering, see explanation of these approaches in section 2.2.1. In Figs. A1 and A2 below, we evaluate the slicing approximation by comparing duration curves of the representative time series with the average output of individual slices. However, note that the curves are sorted individually, and therefore points on the blue and orange curves that appear close to each other do not necessarily originate from the same time periods. Nevertheless, the general shape of the duration curves is approximated well, especially for slicing using k-means clustering. Fig. A3 illustrates typical results of the clustering algorithm.

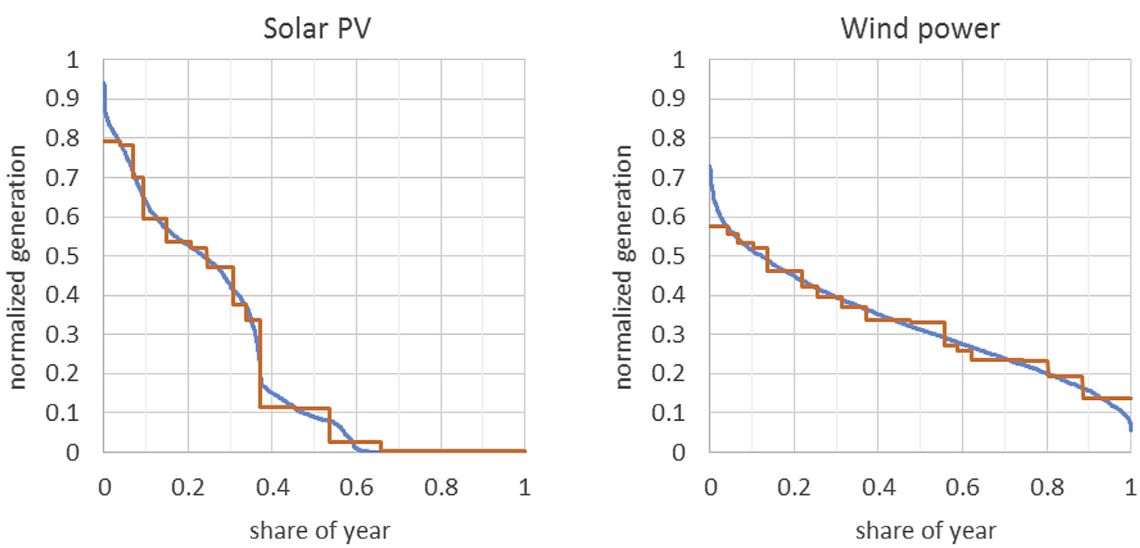


**Fig. A1.** Normalized duration curves of the representative time series for solar PV and wind power in Europe (blue) and sorted average output of the 16 individual slices using k-means clustering (orange).

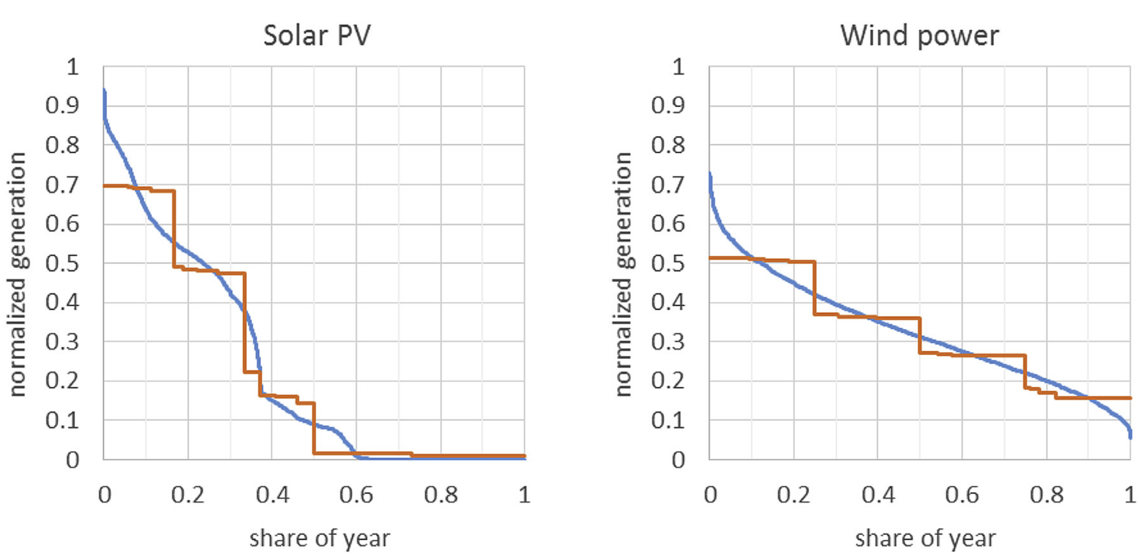


**Fig. A2.** Normalized duration curves of the representative time series for solar PV and wind power in Europe (blue) and sorted average output of the 16 individual slices using 4 × 4 manual slicing (orange).

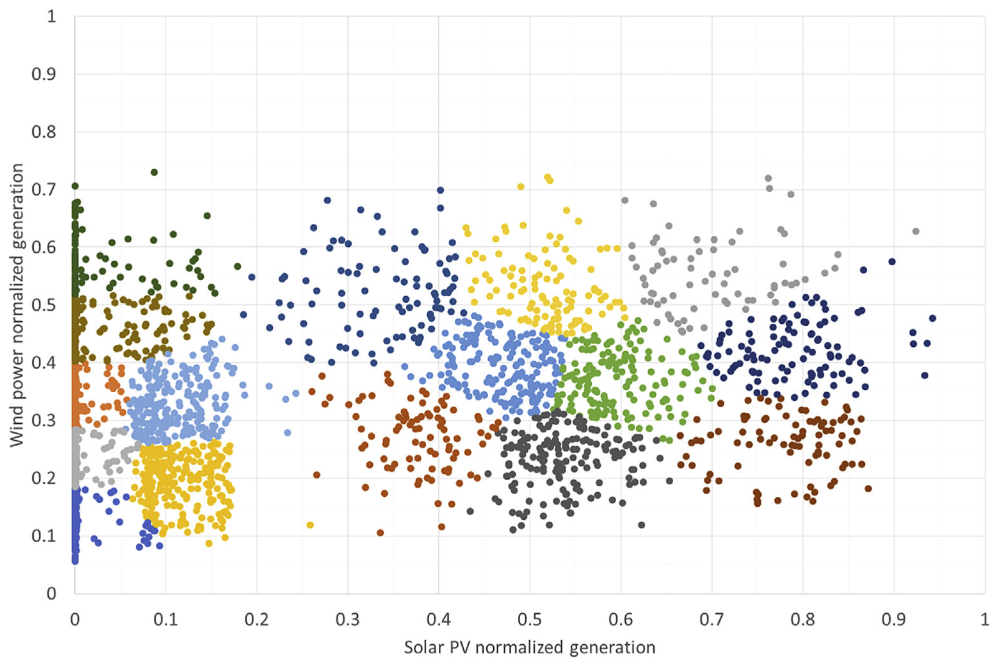


**Fig. A3.** Two-dimensional distribution of normalized representative time series for solar PV and wind power in Europe, coloured using the results of k-means clustering with 16 slices.

*Modelling storage*

As high penetration of variable renewables increases the variability of electricity prices, storing electricity and releasing it during times of high demand or low variable infeed is likely to become an attractive feature of the energy system. Unfortunately most of the time information is lost in the slicing approach we explore, which complicates the modelling of electricity storage. However, some information relevant for operation of storage can be regained by analysing the original wind and solar data at high time resolution. Every storage technology has a characteristic storage time, sometimes called the energy-to-power ratio. For every hour of wind and solar resource data, we look ahead a number of hours corresponding to the characteristic storage time and note the time slice each hour was allocated to. This results in the number of hours per year that an electricity transfer between pairs of time slices is possible, which can be interpreted as a capacity factor for the storage technology for energy transfer between these slices. To illustrate the concept: suppose we have a 12-h storage technology and are interested in how slice X can interact with other slices. We iterate over all time periods in a year and count which other slices appear within 12 h after every occurrence of slice X. When averaged over a year, this gives an upper bound for the number of hours the storage technology can be used to transfer from slice X to any other slice. The model can then choose to build storage capacity if it is cost effective overall. This method is similar to the transition matrix approach proposed by Wogrin et al. [28].

In our model we study four different lengths of storage: 12, 24, 48 and 96 h. The costs for storage are based on the cost data for pumped hydro storage obtained from Zakeri and Syri [30]. Longer storage times were also explored, but found to be uneconomical due to high costs and low utilization.

## Appendix B. Definition of regions

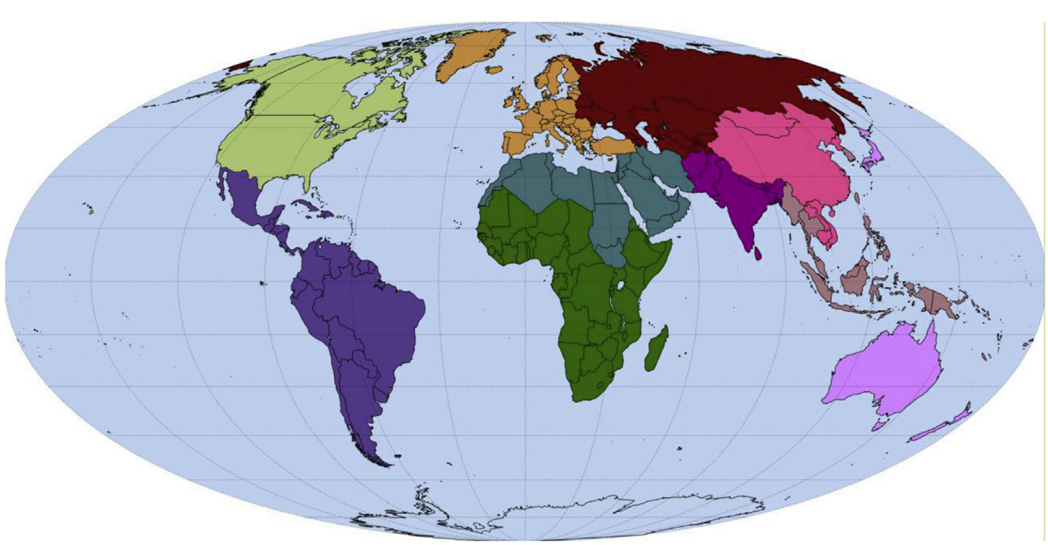

**Fig. B1.** Region definitions in the GET 9.0 model.

**Sub-Saharan Africa (AFR)**: Angola, Benin, Botswana, British Indian Ocean Territory, Burkina Faso, Burundi, Cameroon, Cape Verde, Central African Republic, Chad, Comoros, Cote d'Ivoire, Congo, Djibouti, Equatorial Guinea, Eritrea, Ethiopia, Gabon, Gambia, Ghana, Guinea, Guinea-Bissau, Kenya, Lesotho, Liberia, Madagascar, Malawi, Mali, Mauritania, Mauritius, Mozambique, Namibia, Niger, Nigeria, Reunion, Rwanda, Sao Tome and Principe, Senegal, Seychelles, Sierra Leone, Somalia, South Africa, Saint Helena, Swaziland, Tanzania, Togo, Uganda, Zaire, Zambia, Zimbabwe.

**Centrally planned Asia and China (CPA)**: Cambodia, China (incl. Hong Kong), Korea (DPR), Laos (PDR), Mongolia, Viet Nam.

**Europe (EUR)**: Albania, Andorra, Austria, Azores, Belgium, Bosnia and Herzegovina, Bulgaria, Canary Islands, Channel Islands, Croatia, Czech Republic, Cyprus, Denmark, Faeroe Islands, Estonia, Finland, France, The former Yugoslav Rep. of Macedonia, Germany, Gibraltar, Greece, Greenland, Hungary, Iceland, Ireland, Isle of Man, Italy, Latvia, Lithuania, Liechtenstein, Luxembourg, Madeira, Malta, Monaco, Montenegro, Netherlands, Norway, Poland, Portugal, Romania, San Marino, Serbia, Slovak Republic, Slovenia, Spain, Sweden, Switzerland, United Kingdom, Turkey.

**Former Soviet Union (FSU)**: Armenia, Azerbaijan, Belarus, Georgia, Kazakhstan, Kyrgyzstan, Republic of Moldova, Russian Federation, Tajikistan, Turkmenistan, Ukraine, Uzbekistan (the Baltic republics are in the Europe region).

**Latin America and the Caribbean (LAM)**: Antigua and Barbuda, Argentina, Bahamas, Barbados, Belize, Bermuda, Bolivia, Brazil, Chile, Colombia, Costa Rica, Cuba, Dominica, Dominican Republic, Ecuador, El Salvador, French Guyana, Grenada, Guadeloupe, Guatemala, Guyana, Haiti, Honduras, Jamaica, Martinique, Mexico, Netherlands Antilles, Nicaragua, Panama, Paraguay, Peru, Saint Kitts and Nevis, Santa Lucia, Saint Vincent and the Grenadines, Suriname, Trinidad and Tobago, Uruguay, Venezuela).

**Middle East and North Africa (MEA)**: Algeria, Bahrain, Egypt (Arab Republic), Iraq, Iran (Islamic Republic), Israel, Jordan, Kuwait, Lebanon, Libya/SPLAJ, Morocco, Oman, Qatar, Saudi Arabia, Sudan, Syria (Arab Republic), Tunisia, United Arab Emirates, Yemen.

**North America (NAM)**: Canada, Guam, Puerto Rico, United States of America, Virgin Islands.

**Pacific OECD (PAO)**: Australia, Japan, New Zealand.

**Other Pacific Asia (PAS)**: American Samoa, Brunei Darussalam, Fiji, French Polynesia, Gilbert-Kiribati, Indonesia, Malaysia, Myanmar, New Caledonia, Papua, New Guinea, Philippines, Republic of Korea, Singapore, Solomon Islands, Taiwan (China), Thailand, Tonga, Vanuatu, Western Samoa.

**South Asia (SAS)**: Afghanistan, Bangladesh, Bhutan, India, Maldives, Nepal, Pakistan, Sri Lanka.

## References

[1] J. Rogelj, et al., Emission pathways consistent with a 2°C global temperature limit, Nat. Clim. Change 1 (8) (2011) 413–418.
[2] Climate Analysis Indicator Tool. World Resources Institute.
[3] H.-H. Rogner, et al., Chapter 7-energy resources and potentials, in: Global Energy Assessment - toward a Sustainable Future, Cambridge University Press, Cambridge, UK and New York, NY, USA, 2012, pp. 423–512 and the International Institute for Applied Systems Analysis, Laxenburg, Austria.
[4] IEA, World Energy Outlook 2016, 2016.
[5] P. Nahmmacher, Schmid, Hirth, Knopf, Carpe diem: a novel approach to select representative days for long-term power system modeling, Energy 112 (2016) 430–442, http://dx.doi.org/10.1016/j.energy.2016.06.081.
[6] F. Hedenus, et al., Cost-effective energy carriers for transport - the role of the energy supply system in a carbon-constrained world, Int. J. Hydrogen Energy 35 (10) (2010) 4638–4651.
[7] G. Luderer, et al., The role of renewable energy in climate stabilization: results from the EMF27 scenarios, Clim. Change 123 (3–4) (2014) 427–441.
[8] M. Lehtveer, F. Hedenus, Nuclear power as a climate mitigation strategy–technology and proliferation risk, J. Risk Res. 18 (3) (2015) 273–290.
[9] P. Sullivan, V. Krey, K. Riahi, Impacts of considering electric sector variability and reliability in the MESSAGE model, Energy Strategy Rev. 1 (3) (2013) 157–163.
[10] J.P. Deane, et al., Soft-linking of a power systems model to an energy systems model, Energy 42 (1) (2012) 303–312.
[11] S. Ludig, et al., Fluctuating renewables in a long-term climate change mitigation strategy, Energy 36 (11) (2011) 6674–6685.
[12] K. Poncelet, et al., Impact of the level of temporal and operational detail in energy-system planning models, Appl. Energy 162 (2016) 631–643.
[13] F. Ueckerdt, et al., Representing power sector variability and the integration of variable renewables in long-term energy-economy models using residual load duration curves, Energy 90 (2015) 1799–1814.
[14] C. Azar, K. Lindgren, B.A. Andersson, Global energy scenarios meeting stringent CO2 constraints - cost-effective fuel choices in the transportation sector, Energy Policy 31 (10) (2003) 961–976.
[15] IIASA, GGI Scenario database.
[16] C. McGlade, P. Ekins, The geographical distribution of fossil fuels unused when limiting global warming to 2 [deg]C, Nature 517 (7533) (2015) 187–190.
[17] H. Holttinen, et al., Design and Operation of Power Systems with Large Amount of Wind Power: Final Summary Report, IEA, Espoo, Finland, 2013.
[18] Consumption Data - Hourly Load Values, ENTSO-E - European Network of Transmission System Operators for Electricity, 2014.
[19] M.C. Brower, et al., A Study of Wiind Speed Variability Using Global Reanalysis Data, AWS Truepower, 2013.
[20] D.P. Dee, et al., The ERA-Interim reanalysis: configuration and performance of the data assimilation system, Q. J. R. Meteorological Soc. 137 (656) (2011) 553–597.
[21] CIESIN, Gridded Population of the World, Version 4 (GPWv4): Population Count Adjusted to Match 2015 Revision of UN WPP Country Totals, NASA Socioeconomic Data and Applications Center (SEDAC), Palisades, NY, 2015 (Columbia University).
[22] M.A. Friedl, et al., MODIS Collection 5 Global Land Cover: Algorithm Refinements and Characterization of New Datasets, 2001-2012, Collection 5.1 IGBP Land Cover, Boston University, 2010.
[23] World Database on Protected Areas User Manual 1.3, UNEP-WCMC, 2016.
[24] C. Amante, B.W. Eakins, ETOPO1 1 Arc-minute Global Relief Model: Procedures, Data Sources and Analysis. NOAA Technical Memorandum NESDIS NGDC-24, National Geophysical Data Center NOAA, 2009.
[25] Gridded Dataset of Gross Domestic Product 2010, UNEP/DEWA/GRID-Geneva, 2012.
[26] D. Arthur, S. Vassilvitskii, k-means++: the advantages of careful seeding, in: Proceedings of the Eighteenth Annual ACM-SIAM Symposium Discrete Algorithms, Society for Industrial and Applied Mathematics, 2007.
[27] Matlab online documentation of the k means function [cited 2017 14/6]; Available from: https://se.mathworks.com/help/stats/kmeans.html#bueq7aj-5.
[28] S. Wogrin, et al., A new approach to model load levels in electric power systems with high renewable penetration, IEEE Trans. Power Syst. 29 (5) (2014) 2210–2218.
[29] N. Höhne, M. den Elzen, M. Weiss, Common but differentiated convergence (CDC): a new conceptual approach to long-term climate policy, Clim. Policy 6 (2) (2006) 181–199.
[30] B. Zakeri, S. Syri, Erratum: electrical energy storage systems: a comparative life cycle cost analysis, Renew. Sustain. Energy Rev. 42 (2015) 569–596. Renewable and Sustainable Energy Reviews, 2016. 53: pp. 1634–1635.
[31] MIT, The Future of the Nuclear Fuel Cycle: an Interdiciplinary MIT Study, 2011.
[32] F. Ueckerdt, et al., System LCOE: what are the costs of variable renewables? Energy 63 (2013) 61–75.
[33] L. Hirth, F. Ueckerdt, O. Edenhofer, Integration costs revisited - an economic framework for wind and solar variability, Renew. Energy 74 (2015) 925–939.
[34] G. Pleßmann, P. Blechinger, How to meet EU GHG emission reduction targets? A model based decarbonization pathway for Europe's electricity supply system until 2050, Energy Strategy Rev. 15 (2017) 19–32.
[35] A.E. MacDonald, C.T. Clack, A. Alexander, A. Dunbar, J. Wilczak, Y. Xie, Future cost-competitive electricity systems and their impact on US CO2 emissions, Nat. Clim. Change 6 (5) (2016) 526–531.
[36] F. Ueckerdt, R. Pietzcker, Y. Scholz, D. Stetter, A. Giannousakis, G. Luderer, Decarbonizing global power supply under region-specific consideration of challenges and options of integrating variable renewables in the REMIND model, Energy Econ. 64 (2017) 665–684.
[37] B. Ridley, J. Boland, P. Lauret, Modelling of diffuse solar fraction with multiple predictors, Renew. Energy 35 (2) (2010) 478–483.
[38] P.G. Loutzenhiser, et al., Empirical validation of models to compute solar irradiance on inclined surfaces for building energy simulation, Sol. Energy 81 (2) (2007) 254–267.
[39] Global wind Atlas, DTU Wind Energy, 2016.
[40] J. Olauson, M. Bergkvist, Modelling the Swedish wind power production using MERRA reanalysis data, Renew. Energy 76 (2015) 717–725.
[41] C. Moné, et al., 2014 cost of Wind Energy Review, NREL, 2015.